Chapter 1

Nanoscale Cutting

1.1. Introduction

In nano and micromachining processes the actual material removal can be limited to the surface of the workpiece, i.e. only a few atoms or layers of atoms. At this range, inherent measurement problems and the lack of more detailed experimental data limit the possibility for developing analytical and empirical models as more assumptions have to be made. On the basis of atomistic contact models, the dynamics of the local material removal process and its impact on the material structure, as well as the surface generation, can be studied.

The first pioneering applications in molecular dynamics (MD) indentation and material removal simulation were published between 1989 and 1991 [BEL 91, IKA 91, HOO 90, LAN 89]. By starting at the atomic level, the considered microscopic material properties and the underlying constitutive physical equations of state in MD provide, in principle, a sufficiently detailed and consistent description of the micromechanical and thermal state of the modeled material to allow for the investigation of the local tool tip/workpiece contact dynamics [HOO 91, RAP 95]. The description of microscopic material properties considers, e.g., the microstructure, lattice constants and orientation, chemical elements and the atomic interactions.

Chapter written by Rüdiger RENTSCH.

The more universal material representation in MD further allows us to go beyond ideal, single crystalline structures and to also consider polycrystals, defect structures, pre-machined or otherwise constrained workpiece models and non-smooth surfaces [DAW 84, REN 95-1, REN 95-3, YIP 89]. Various application-specific boundary conditions may be applied [HOO 91, RAP 95, YIP 89]. In recent years the number of applications considering quantum mechanics for the interactions between atoms has been steadily increasing. However, here only the more classical atomistic approach will be presented.

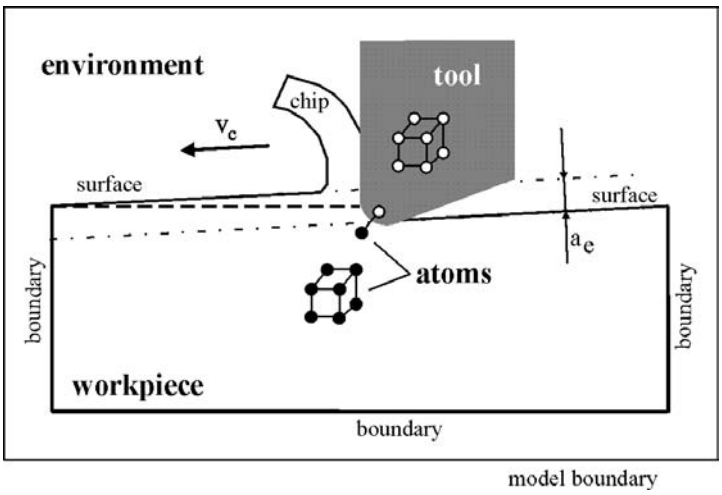

Figure 1.1. *Concept of a molecular dynamics cutting model setup*

Figure 1.1 shows a general description of an often applied concept for MD cutting process simulation, i.e. the orthogonal cutting condition, and includes the essential elements of MD modeling. In addition to the material properties and the interactions between its constituents, the contact and interface conditions, e.g. between tool tip and workpiece as well as with their environment, need to be described. Furthermore, the boundary conditions within the model (surfaces vs. bulk material) and the system boundaries to the non-modeled environment are of importance. Table 1.1 provides a list of the necessary physical elements and principles as well as their area of application in MD modeling. The mathematical description of the equation of motion in particular has been included in this listing, since its choice has a major influence on the numerical complexity and the accuracy of calculation.

In respect of the application of MD modeling for the nanoscale cutting process simulation, in the following chapter some of the basic elements in Table 1.1 will be described in more detail first. Then, in section 1.3, the design and requirements for state-of-the-art MD cutting process simulations will be discussed and, in the following section, the capabilities of MD for the nanoscale material removal process analysis will be demonstrated on the basis of results of application examples. Some aspects regarding significant advances and recent developments in MD material removal process simulation will be discussed in section 1.5, before the summary and outlook of this contribution is given.

Physical element/ principle	**Application in MD**
• microstructure	initial configuration
• micro-mechanics	atomic interaction
• dynamics	equation of motion
• mathematical description	numerical integration (dynamics)
• thermodynamics	energy balance of the system
• boundary conditions	micromechanical boundaries of the model

Table 1.1. *Application area of the physical elements and principles in MD modeling*

1.2. Basic elements of molecular dynamics modeling

1.2.1. *Material representation and microstructure*

While the original molecular dynamics theory is well based within physics, empirical elements were introduced from the materials science field in order to match the results of experiments with the theoretical and so far physical model. The key to computational efficiency of atomic-level simulations lies in the description of the interactions between the atoms at the atomistic instead of the electronic level. This reduces the task of calculating the complex many-body problem of interacting electrons and nuclei as in quantum mechanics to the solution of an energetic relation involving, basically, only atomic coordinates [HOO 91]. Accordingly, a discrete body or a certain material is described by its chemical elements and by their coordinates. The coordinates provide the information about the atomic arrangement, i.e. the structure of the material, which could be set up, e.g. for a metal on the basis of known lattice structures and lattice constants.

The atomic arrangements in Figure 1.1 hint at the requirement of a description for all matter involved, primarily for the workpiece and the tool material. Considering the crystal size of typical metals, which range between a few tens to several hundred microns in diameter, single crystalline workpiece structures represent reasonable material structures for nanoscale cutting simulations as the tool tip will have to cut over a length of at least 30,000 unit cells before reaching a grain boundary area. However, defects in crystalline structures, like grain boundaries and dislocations [DAW 84, REN 95-3, REN 06, SHI 94, YIP 89], amorphous materials [GLO 95, RAP 95] or polymers as well as liquids and gases [ALL 87, RAP 95] can also be studied using MD. Although Figure 1.1 shows a 2D orthogonal cutting setup, the choice of material representation should always be 3D, even if the width of the model is chosen to be only one unit cell wide. The advantage of 2D models lies in the reduced calculation time and a somewhat easier visualization of the results. However, these advantages are combined with many disadvantages and a great loss of information and meaning of carrying out atomistic simulations. With pure 2D models it is impossible to sufficiently describe the 3D crystalline structure of metals and, hence, no realistic slip system or dislocation motion seems possible and no realistic deformation behavior can be expected. Because of the missing third dimension, 2D simulations result in enhanced, deeper deformation slip as atoms are constrained to accommodate within a plane, in opposition to a 3D model, where each atom has an additional degree of freedom (DoF) to store energy in space [REN 01].

1.2.2. *Atomic interaction*

The central element of the MD code is the calculation of the particle-particle interactions. As it is the most time-consuming part in an MD computer program, it determines the whole structure of the program. Efficient algorithms for the calculation of the interaction are important for systems with a large number of atoms (see [ALL 87, RAP 95]).

The interactions between particles are specified by functions that describe the potential energy. Depending on the complexity of a material and the chosen mathematical description respectively, the potential function may consider many parameters. The goal of the potential function development is that the functional description and the material-specific set of parameters lead to a self-organizing, known structure as a function of the state variables. This provides the basis as well as the necessary flexibility for carrying out not only phase and structure calculations, but also cutting process calculations at the nanoscale. Potential functions and sets of parameters have to be specified for all possible combinations of interactions that need to be considered. In the following, the principles of the necessary potential functions will be described using the widely applied so-called pair potential

functions. The class of the more complex many-body potentials, which is of more importance for the representation of metals, will however be discussed only briefly.

1.2.2.1. *Pair potentials*

First, van der Waals described a model of a material which can form liquid and solid condensed phases at low temperatures and high pressures. Such condensed phases require both attractive and repulsive forces between atoms [HOO 91]. Since the simplest possible representation of many-body interactions is a sum of two-body interactions, the so-called pair potentials were the first potential descriptions of this type. A typical course of the functions is shown in Figure 1.2.

The best known pair potential functions are the Lennard-Jones and the Morse potentials (see equation [1.1] and equation [1.2]) for which the potential energy Φ is only a function of the separation or bonding distance $|r|$ between two atoms. The well-depth of the functions are given by parameters ε and D for the minimum potential energy or sublimation energy, while σ and r_o are constants that define the position of the energy minimum. These parameters are derived from fitting to experimental data like lattice constants, thermodynamic properties, defect energies and elastic moduli. The interaction forces can be derived by calculating the derivative of the potential function, for the pair potential functions only with respect to the separation distance $|r|$.

Lennard-Jones: $$\Phi_{LJ}(r) = 4 * \varepsilon * [(\sigma / r)^{12} - (\sigma / r)^{6}] \quad [1.1]$$

Morse: $$\Phi_{M}(r) = D * [e^{-2\alpha(r-ro)} - 2e^{-\alpha(r-ro)}] \quad [1.2]$$

The potentials describe chemically active materials as bonds that can be established or cut at the long-range part. They represent reasonable descriptions for two-body forces to the extent that they account for the repulsion due to overlapping electron clouds at close distance and for attraction at large distances due to dispersion effects. Generally in solids a shielding effect is expected to make interactions beyond the first few neighbors of limited physical interest. Thus, potential functions are commonly truncated at a certain cutoff distance, preferably with a smooth transition to zero (see Figure 1.2), and result in so-called short-range forces. In addition, the long-range Coulomb forces are usually beyond the reach of MD model sizes [HOO 91].

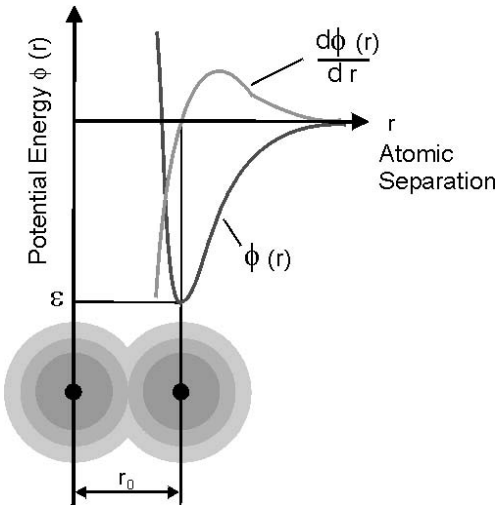

Figure 1.2. *Potential energy according to atomic separation*

1.2.2.2. *Many-body potentials*

The simplicity of the pair potential functions make them appear attractive, for many-atom systems in particular, but they only stabilize structures with equal next neighbor distances, like fcc and hcp structures, basalt planes and triangular lattices. However, using pair-potentials it is not possible to correctly describe all elastic constants of a crystalline metal. For a better representation of metals, many-body interactions need to be included into the function as for example in the well-known potentials following the embedded atom method (EAM) [DAW 84, FIN 84]. In all of the following MD results, the Finnis-Sinclair-type EAM potential by Ackland *et al.* was employed for the workpiece-workpiece interactions [ACK 87]. EAM potentials have been developed and tested for complex problems such as fracture, surface reconstruction, impurities and alloying problems in metallic systems.

The structure of brittle or non-metallic materials with, for instance, covalent or ionic bonds can also not be satisfactorily described by simple pair-potentials. Ionic materials require special treatment because Coulomb interactions have poor convergence properties unless the so-called periodic boundaries are implemented with care (see [ALL 87]). For the diamond lattice or the similar cubic zinc blend structure of covalently bonded semi-conductors like silicon and germanium as well as some ceramics, it is necessary to treat the strong directional bonding explicitly by including terms that describe the interaction between three or more atoms considering bond angles and bond order (see [TER 90, YIP 89]).

1.2.3. *System dynamics and numerical description*

Molecular dynamics comprises macroscopic, irreversible thermodynamics and reversible micro-mechanics. The thermodynamic equations form a link between the micromechanical state, a set of atoms and molecules, and the macroscopic surroundings, the environment. The thermodynamic equations yield the quantities, system temperature and hydrostatic pressure of the model and allow us to determine energy changes involving heat transfer. In mechanics, it is usual to consider energy changes caused by displacement and deformation. By the term "mechanical state" of a microscopic system we mean a list of present coordinates (r) and velocities (v) of the constituents [HOO 91]. For this information about the state of the system to be useful, equations of motion, capable of predicting the future, must be available. As the governing equations of motion for a system of constant total energy, the well-known Newton's equations of motion can be chosen:

$$\text{Newton's equations of motion } d\{v_i(t)\} / dt = 1 / m_i * \Sigma_{i<j}\{F_{ij}(r_{ij},\alpha,...)\} \qquad [1.3]$$

$$d\{r_i(t)\} / dt = v_i(t) \qquad [1.4]$$

with i,j = 1 to n.

The resulting force on an atom i is expressed by an integral over all force contributions F_{ij}. Numerically this is calculated as a sum over all forces acting on each atom i (equation [1.3]). Hence, two bodies at close distance interact through this sum of force contributions in the equation of motion. To advance the atoms in space, the equation of motion has to be integrated with respect to time, once to obtain the new velocity and twice for the new position of each atom. Numerically, this operation is more efficiently carried out by approximation schemes, for instance using finite difference operators and the so-called Verlet or Stoermer algorithm [ALL 87, HOO 91]:

$$\text{Verlet algorithm: } r_i(t+\Delta t) = r_i(t) + \Delta t * v_i(t) + 1/(2*m_i) * \Delta t^2 * F_i(t) \qquad [1.5]$$

$$v_i(t+\Delta t) = v_i(t) + \Delta t /(2*m_i) * \{F_i(t+\Delta t) + F_i(t)\} \qquad [1.6]$$

with i = 1 to n.

With the present positions ($r_i(t)$), velocities ($v_i(t)$) and forces ($F_i(t)$), first the new positions and forces at time $t+\Delta t$ and then the new velocity can be calculated. Given the equations of motion, forces and boundary conditions, i.e. knowing the current mechanical state, it is possible to simulate the future behavior of a system. Mathematically, this represents an initial value problem. A reasonable distribution of the initial velocities can be obtained from the Maxwell-Boltzmann distribution function.

The dynamic development of the atomic system as a whole determines the instantaneous kinetic state of the system. By relating the average kinetic energy of the atoms (with average velocity v), i.e. their micromechanical state, to the thermal energy of the system, which is the thermodynamic state, the gas kinetic definition of the system temperature is adopted. From equation [1.7], the temperature T of a 3D system of atoms can be directly observed or, for a given reference temperature, the kinetic energy in the system can be controlled (for details see [ALL 87, HOO 91]).

$$E_{kin} = {}^{1}/_{2} * m * {}^{1}/_{n} * \Sigma v_i^2 = {}^{3}/_{2} * k_B * T = E_{therm.} \qquad [1.7]$$

with i = 1 to n.

Since the initial choice of the atom configuration is more or less idealistic, i.e. artificial, it does not fit into the Maxwell-Boltzmann distribution from the energetic point of view. The whole system needs to pass through an initial equilibration phase, during which the atom configuration adjusts to the invariants of the system, e.g. total system energy, volume, pressure and/or temperature, and thereby also to the boundary conditions.

1.2.4. *Boundary conditions*

Boundaries are an intrinsic, vital part of models. Thermodynamic properties are thought of as characterizing “bulk” matter, which represents enough material so that surface effects and fluctuations can be ignored. To decrease the influences of boundaries, the system size needs to be chosen to be “big enough” [HOO 91]. However, the fulfillment of this weak requirement is generally limited by the available CPU power and time.

In addition to the option of free surfaces, which would result in a particle cluster in free space if applied to all axes of a Cartesian coordinate system, basically two types of boundaries are common in MD simulations: fixed and periodic boundaries. The simplest type, in terms of realization, is the fixed atom boundary which confines all freely propagating atoms inside a closed box of non-moving atoms or provides support for them at one or more sides. It is simply realized by taking away the dynamics of such boundary atoms, but keeping the interactions with the freely moving atoms. The consequences of such infinitely hard boundaries for the simulation can be significant as no energy can be passed through the boundary and phonons will be reflected at it. The sole use of hard boundaries represents a poor representation of the surrounding environment/material. Some of the negative effects of hard boundaries can be corrected by placing thermally controlled atom layers between freely moving atoms and a hard boundary [BEL 91, SHI 92].

Periodic boundary conditions (PBCs) were introduced to avoid the hard boundary reflection and allow us to study bulk and bulk/interface structures without the strong boundary influence in small models (see [ALL 87, HOO 91]). It is imagined that the bulk of the material is made of many similar systems along the axis perpendicular to the periodic boundary plane, i.e. there are no surfaces along this axis. The system reacts as if there are identical systems at both sides of the PBC, exposed to the same conditions and changes (see Figure 1.3). In practice, the system is connected to itself, and atoms at one side interact with atoms on the other side and form a continuous structure. If deformation in the system requires an atom to slip across the PBC, it transfers from one side of the model to the other. Figure 1.3 shows a sketch of an indentation model (triangular indenter on the top of a work-piece), where a one-axis PBC is considered perpendicular to the horizontal axis.

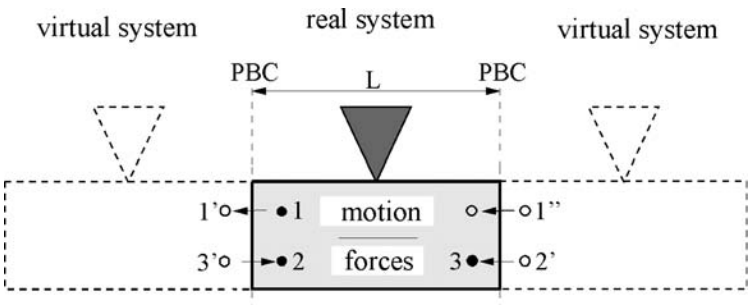

Figure 1.3. *Motion through (atom 1) and forces at (atoms 2-3) a PBC*

A consequence of periodic boundaries is that energy and phonons are not reflected, but travel through the system by means of the PBCs. One or two-axis PBCs can be employed where symmetry axes are available and the lattice structure allows an undisturbed bonding through the PBC planes. Additionally, a deformation compatibility across a PBC has to be fulfilled by an appropriate alignment of preferred slip systems relative to the PBCs, in order to avoid artificial deformation patterns.

The following results were all obtained by using 3D MD models, EAM potential functions and PBCs in one or two axes, even if the width of the underlying MD model was only a few lattice constants wide, following the approach of the orthogonal cutting process condition.

1.3. Design and requirements for state-of-the-art MD cutting process simulations

The fundamental part of a material removal process is the relative motion of two interacting bodies, where one is carrying out work, usually the tool, upon the other one, the workpiece. Therefore, the MD model needs to include, at least, the surfaces of these two interacting bodies in the area of contact and a sufficient portion of matter (see Figure 1.4). Hence, full 3-axis PBCs are not applicable since the surfaces have to be along one axis. Furthermore, a relative motion between both bodies needs to be applied to account for the cutting speed. The process requires that cutting, thrust and tool forces are balanced or accommodated at the system boundaries in order to measure, for instance, tool forces or to avoid unintended translational and rotational motion by the tool or the workpiece as a whole.

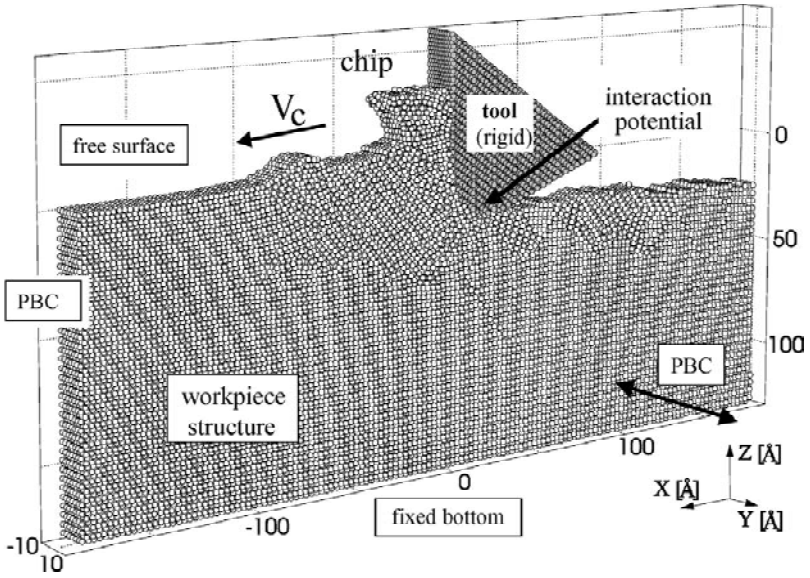

Figure 1.4. *Design and boundary conditions of a 3D MD cutting model*

In most cases the cutting process simulations focus on the effect of the material removal process on the workpiece structure, for which the tool is often modeled rigid in order to reduce the complexity of the simulation as a whole. By exerting work with the hard tool tip upon the workpiece, energy is added to the workpiece, whereupon its temperature would rise. Implementing the earlier mentioned thermally controlled atom layers around the outer boundaries of the workpiece allows us to control its temperature by drawing away energy to the non-modeled

area of an imagined larger workpiece volume [BEL 91, SHI 92]. Although in the literature results from MD simulations of the machining of brittle semi-conductor and of ductile polycrystalline materials have also been presented ([GLO 93, GLO 95, REN 95-1, REN 95-3, SHI 94]), all the following figures, like Figure 1.4, show results of cutting or machining process simulations where hard tool tips move on {001} surfaces along <110> directions of fcc copper crystals.

The machining operation represents a massive deformation process. In order to reduce interactions with the boundaries and to allow for sufficient elastic deformation, a reasonably large-sized model has to be determined by tests or on the basis of experience. Experience further shows that 2D MD models have little meaning, unless the process in question is restricted to a plane and all important information can be accounted for in such a model. In most cases a 3D model or at least a semi- or quasi-2D model is the better choice, since material properties and structures are significantly better represented.

The relative motion for the material removal process can either be applied to the tool tip model or the boundary atoms of the workpiece (the freely moving atoms follow automatically). When the tool tip comes into contact with the workpiece surface, the deformation causes material to be piled up in front of the tool tip whereupon gradually a chip is formed during the course of process simulation. To reach constant cutting conditions it is necessary to observe the process and its quantities for a sufficiently long time as it will be discussed in the next chapter in more detail. For both requirements, sufficiently large model sizes as well as long process observations, the use of fast and large computing systems, like parallel-processor computers, is as desirable for MD as fast algorithms. Regarding fast algorithms, the basic idea of the introduced techniques is to reduce the calculation of forces and stresses to those that are necessary. In principle, the force calculation is at least an N^2 operation, even for simple pair potentials. Methods to speedup the calculation, like the so-called book-keeping technique, the next-neighbor-cell method [ALL 87] or the use of tabulated force functions [REN 95-1], employ static or dynamic tables at different levels of the calculation procedure. Using these techniques, the program codes become significantly more complex, but change the dependence of the calculation time on the system size from an N^2 relation to an N^1 relation. Further details about these techniques can be found in the literature [ALL 87, REN 95-1].

1.4. Capabilities of MD for nanoscale material removal process analysis

For the analysis of the MD process simulation results, micromechanical state variables of all atoms and the thermodynamic state variables of the system as a whole are accessible throughout the simulation. While some of the state variables are directly available, like coordinates and velocities ("micromechanical state"), others are only available through statistical mechanics, which need to be calculated as system quantities like the thermodynamic state variables heat, temperature and pressure.

Some of the capabilities of MD for analyzing nanoscale cutting processes by simulation will be demonstrated on the basis of application examples. For this purpose results of orthogonal cutting process simulations of a ductile, single-crystalline copper will mostly be presented, although MD cutting and machining simulation results of brittle as well as ductile polycrystalline materials can be found in the literature [GLO 93, GLO 95, REN 95-1, REN 95-3, SHI 94]. If not otherwise stated, all the following figures show results of cutting or machining process simulations where hard tool tips move on {001} surfaces along <110> directions of fcc crystals.

1.4.1. *Analysis of microstructure and deformation*

The direct availability of the atom coordinates in MD calculations allows us to visualize the instantaneous positions and to track the motion of the atoms individually as well as a whole. This information is not only useful for so-called snapshots of atom arrangements as shown in Figure 1.4, through which the progress of process simulation can be monitored, but it can be used for dynamic analyses on the basis of animations as well. For this purpose the radii of the atoms are often chosen more in order to enhance a certain aspect or view of a specific arrangement than representing realistic atom sizes. Using instantaneous coordinates rather than averaged positions, due to the vibration of the atoms, does not cause a significant error, because usually the maximum vibration amplitude of an atom in a stable MD calculation is less than 1% of the minimum bonding length.

The model in Figure 1.4 was employed to study the chip formation process and the surface generation at a cutting edge in nanoscale cutting. By employing 1D PBC along the y axis, the orthogonal cutting condition reduced the model to a quasi-2D type with a small width, which makes it possible to correctly model the 3D fcc crystal structure of the copper workpiece as well. The model contained 71,000 work atoms and 11,000 tool atoms. Atoms at the bottom and to the very left and right hand side of the model represent fixed boundaries, but were shifted with cutting speed to create the relative motion between workpiece and tool. Atoms in the layers

next to these hard boundary atoms had thermostat properties and controlled the temperature at the workpiece boundary.

Since for diamond cutting of copper no plastic and no significant elastic deformation of the tool was expected, calculating its internal structure was not of special importance, but its shape and surface structure were relevant for the tool-work interaction. Its surfaces were formed by preferred diamond/fcc cleavage planes and used as rake and clearance faces. The edge radius was not chosen atomically sharp (here 2 nm), in order to consider limited minimum edge radii, because of surface stresses [IKA 77]. To further provide a reasonable tool-work contact the tool structure had the atomic density of diamond. Although the tool was modeled as a hard body with collectively moving atoms, i.e. no interaction within the tool, the interaction potential between tool and work atoms needed to be specified. Data for the diamond/copper interaction based on a pair potential function were found in Shimada *et al.* [SHI 93]. The cutting forces were calculated as reaction forces at the tool due to its infeed motion into the workpiece surface. The work atom interactions are described by Ackland's EAM potential for copper [ACK 87]. The cutting speed was restricted to 100 m/s and 50 m/s. Lower speeds were not practical to simulate due to computational limitations.

Figure 1.4 shows a single-crystalline structure, which moved towards the cutting tool, whereupon material is deformed in front of the tool tip, the chip generation is initiated and dislocation loops can be identified at the generated workpiece surface. Figure 1.5 shows a so-called deformation graph in a 2D projection of the same model and progress of simulation. It shows areas of plastic deformation, dislocations and large elastic deformations in the subsurface region. The method is based on horizontal and vertical connections between initial-neighbor atoms. Deformations appear as sharp equilateral folds in neighboring layer lines within the otherwise rectangular structure or by narrowing mesh spacing as in the case of strong elastic deformation. For large displacements between initial-neighbor atoms, the bond was considered to be broken and was no longer drawn. In this way, highly deformed areas, like the chip and the newly generated surface, show few initial-neighbor lines.

Deep running dislocations, observed in 2D MD cutting simulations if pair potentials are being used ([REN 95-2, REN 96]), could not be confirmed by employing this 3D model and the better EAM potential. This model predicts intensive plastic deformation at the generated surface with a thickness of only a few atom layers. At the same strain, a 2D model always predicts larger dislocations than its 3D counterpart. The cutting process changes drastically when changing the ratio of cut depth to cutting edge radius from 0.5 to 1.0, also depending on the crystalline orientation of the work. At a ratio of $a_e/r_\beta=1.0$, the tool begins to use its rake face more for the chip formation. With the increase in cut depth, the portion of twin dislocations in chip formation increases over dislocation slipping. Such twinned

areas can be seen ahead of the tool and the chip. The lower energy requirement for twinning makes the chip removal process at larger cut depths more efficient and the cutting forces only increase proportionally.

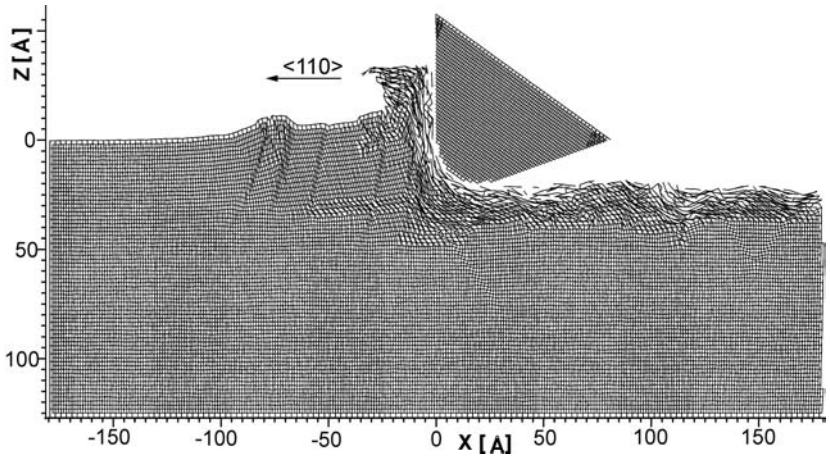

Figure 1.5. *Deformation graph, view <110>*

Figure 1.6 shows two subsequent 2D views of microstructural snapshots of the same model as in Figures 1.4 and 1.5, but at a smaller cut depth than before. Analyzing the changes in the microstructure deepens the understanding of the involved mechanisms of material removal for specific cutting conditions. In Figure 1.6 areas with different crystal orientation are separated by lines and slip lines drawn for identified dislocations. The cutting process right before state a) was characterized by a growth of the pre-deformation area in the cutting direction (ahead of the chip) without an increase in chip length. Until state b) this process had stopped, the pre-deformation area decreased while the chip grew in size. The microstructural plots show a change of the crystal orientation in the chip root area that supports either the deformation away from the chip root (a) or the chip formation in the chip root area.

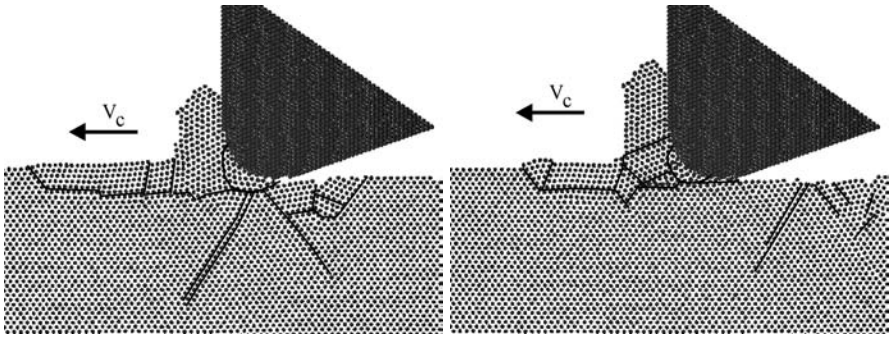

a) 163 ps b) 202 ps

Figure 1.6. *Microstructural changes in the chip root area during chip formation*

1.4.2. *Obtaining cutting forces, stress and temperature*

When modeling systems of discrete particles and observing their progression over time, statistical mechanics provides a basis for the analysis and description of the behavior of such systems. It has been demonstrated for a Gibbs microcanonical ensemble that taking time averages is in statistical agreement with taking phase-space averages and that the numerical quality of results in MD can always be improved by longer calculations [HOO 91].

As mentioned before, cutting forces can be calculated as reaction forces at the tool due to its relative motion during contact with the workpiece atoms. For every time step Δt (see equation [1.3]), which is usually in the range of a few femtoseconds (10^{-15} s), the force contributions of the workpiece atoms interacting with the tool are integrated (see equation [1.5]). The dynamic character of such a system with a large number of degrees of freedom, i.e. all the freely moving workpiece atoms, emerge as fluctuations of derived, non-constant quantities. Figure 1.7 shows the course of the cutting force radio for the simulation in Figure 1.6.

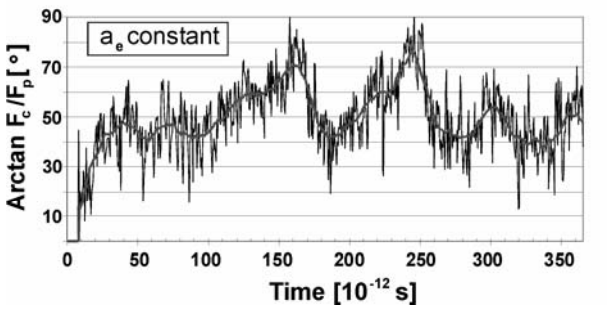

Figure 1.7. *Course of the cutting force ratio Fc/Fp*

The instantaneous tool forces, which will be newly calculated for every time step, fluctuate intensively. Calculating a moving average of the force ratio over 1,000 time steps for example cancels out the fluctuations and leads to a smooth course. After overcoming the equilibration phase (no cutting forces), the first tool/workpiece contact was made and the force ratio changed to an average value of 1 (=arctan 45°) over a period of about 20 pico seconds (10^{-12} s). Besides smaller maxima and minima during the observed total process simulation time, two gradually developing maxima in the course of the force ratio appear at about 165 pico seconds and 245 pico seconds. Figure 1.6 sheds light on the microstructural process which is related to the observed course of the force ratio.

Detailed information about the distribution of stresses and temperature in nano- and microscale cutting are of great interest for science and the manufacturing industry. So far most of the MD results of cutting process simulations were presented as atomic, discontinuous sets of instantaneous data at individual atom sites, such as snapshot atom positions, relative displacement and instantaneous atomic temperature. Besides the limited meaning of instantaneous atomic temperatures and stresses, looking at such large sets of 10,000, 100,000 or even millions of pieces of data is not practical from a point of view of efficient data analysis. Furthermore, it makes any attempt to compare MD results with, for instance, results from continuous mechanics difficult if not impossible. Taking advantage of the possibility of improving the quality of local values by calculating them as time averages over a sufficiently long period of time provides the means to obtain a deeper insight of the model and the simulated process. Thus, aiming at macroscopic thermodynamic properties, suitable time intervals for averaging these properties have to be identified. Simulations showed that an average over about 1,000 time steps led in some cases to sufficiently stable mean properties, but still provides a certain time resolution in order to study details of the process. Considering the basics of MD and the physical nature of these quantities, the results can now be represented in a form of gradual distributions as so-called contour plots,

with a certain resolution in space as well as in time. The representation of stresses and temperature in terms of continuous distributions allows a direct comparison of continuous mechanic results and MD results.

In Figure 1.8 the calculated distribution of the maximum shear stress of the orthogonal cutting process already shown in Figure 1.4 and Figure 1.5 is given. With the help of this distribution it is possible to determine where stress concentrations occur, how much the crystal structure influences the stress distribution, as well as the material removal process, and what the differences are in comparison to macroscopic, continuous mechanical processes.

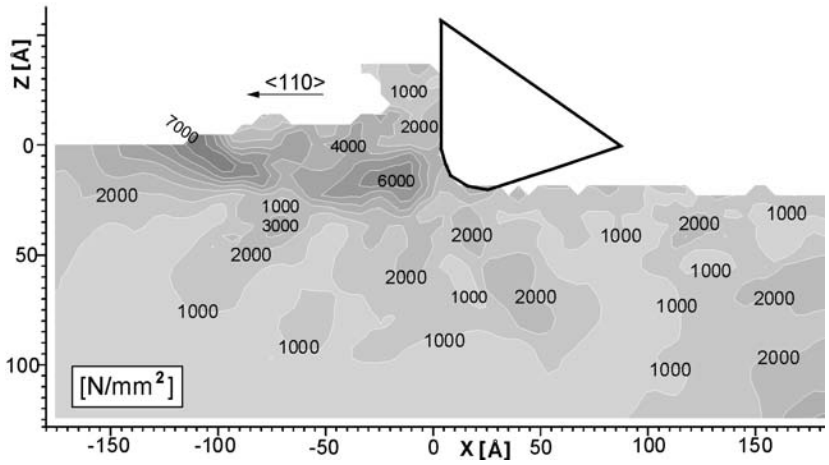

Figure 1.8. *Shear stress distribution in an orthogonal 3D MD machining model*

They also allow us to determine how deeply the process influences the workpiece and where new dislocations can occur, since areas of high shear stress are potential sources for formation or extension of dislocations. Similarly, temperature distributions can also be calculated by adapting equation [1.7] to local volumes and calculating time averages. As it will be shown in the following section (Figure 1.12b), MD cutting process simulations without the consideration of fluids lead to approximately concentric temperature distributions, in which the hottest areas are the chip area and the chip root area. Right at the tip of the tool, the material is deformed at a high stress level, whereby a lot heat is generated. Hence, the high temperature areas extend from the chip under the tip of the tool, as one important source of heat generation, to the areas of shearing. It should be noted here that modeling the tool by rigid, thermally inactive atoms does not enable the tool to

conduct any heat. Therefore, the tool acts like a thermal isolator, which further supports a concentration of heat in the chip.

Regarding the temperature distributions in MD cutting simulations, it should be further noted that in most of the published works, only the thermal conductivity through phonons is considered. Conductivity by electrons is neglected in such cases, even though it is one order of magnitude larger than that of the phonons. Hence, the presented temperature levels as well as the local gradients would actually be lower than shown. New algorithms were developed to describe thermal conductivity more accurately by considering both the electron and phonon conductivity [CAR 94].

1.5. Advances and recent developments in material removal process simulation

In this chapter two aspects of advances and recent developments in material removal process simulation using MD will be explained in more detail. They are the possibility of carrying out complete 3D surface machining simulations and the consideration of fluids.

1.5.1. *Complete 3D surface machining simulation*

For abrasive processes, the model requirements are higher than for cutting processes, since orthogonal symmetry is not given and a quasi-2D model, like in Figure 1.4, cannot be applied. Besides the need to describe the geometry of abrasives, the model has to provide sufficient space for the deformation and chip formation of the 3D material removal process. Figure 1.9a shows a snapshot of a molecular dynamics simulation to study material pile-up and chip formation in abrasive machining as a function of shape and orientation of the abrasives.

The simulation in Figure 1.9 considered two hard pyramidal grits with diamond structure and two different orientations. The figure shows an advanced state of simulated 3D grinding using a model with more than 100,000 copper atoms (the workpiece height was 6 nm). In several ways the simulation represents a high-end state-of-the-art MD simulation of the grit/workpiece contact as the interactions were based on an EAM potential function [ACK 87] and the model considers two abrasives that cut at 100 m/s through a workpiece over its whole length. Thus, the periodic boundaries (for both directions of the horizontal plane) lead to complete groove formation by the grits in cutting direction and describe a model setup with multiple grit/workpiece contacts like in grinding (see Figure 1.9b). By repeating the complete groove generation with relative-to-the-cutting-direction shifted abrasives, the machining of the whole surface can be realized. This provides the basis for 3D surface roughness and residual stress analyses of completely machined surfaces at

realistic machining speeds (common grinding speeds range from about 5 to 80 m/s and high speed grinding up to about 250 m/s).

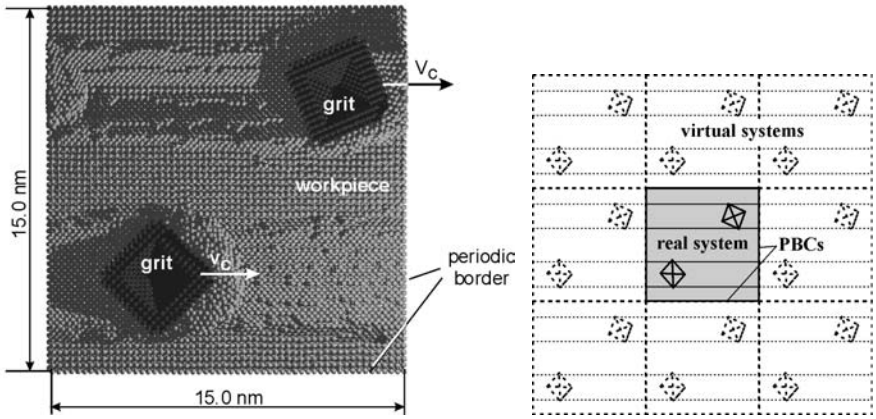

a) MD grinding model (top view) b) Effect of 2D PBC on grinding model

Figure 1.9. *Snapshot of a full length model scratching simulation with 2 hard abrasives (after 360,000 time steps, 144 ps) [BRI 06]*

Thorough analyses of the chip formation, the elastic and plastic response of the workpiece and process quantities in MD simulations have revealed clear and consistent effects. As [REN 96] and [SZE 93] show, for example, the machining speed has a direct influence on the microscopic material removal process and the chip formation in MD simulations. The results suggest that the sensitivity of the simulation results on the machining speed is less strong than observed in experimental investigations. A possible reason for this effect is that the implemented boundary conditions and model settings have a strong impact on the dynamics of the finite process model. However, significant changes in magnitude of the machining speed lead to significant changes in chip shape and formation mechanism. Further quantities of the process are effected, due to an increasing localization of the deformation process at high speeds. More direct effects on the process simulation results show the depth of cut, the grit orientation and the cutting edge radius. Hence, it is possible with MD to simulate the influence of grain shape and orientation on the efficiency of abrasive processes. On the basis of bigger MD models, it will be possible to determine the energy dissipation by a direct analysis of elastic and plastic work and the microscopic mechanisms that determine the surface roughness in nanoscale machining processes.

1.5.2. *Consideration of fluids in MD cutting simulation*

Most state-of-the-art material removal process simulations focus on the material removal mechanisms, chip and surface generation [MAE 95, KOM 99, REN 95-2, SHI 93, SHI 94]. Besides partially strong idealizations of the tool and workpiece properties as well as the direct contact and boundary conditions, so far fluids have not been included in the environmental descriptions of workpiece and tool in MD-modeling. Hence, such an environment represents high vacuum conditions with no heat convection to an atmosphere or coolant. Therefore, an extension of MD machining process simulation has been proposed by considering fluids together with the tool tip and the workpiece [REN 05]. The extension of MD machining process models by molecular gas and fluid dynamics (see [HOO 91, RAP 95]) provide an opportunity for enabling a complete energy balance and for investigating the impact of adsorption and reaction layers at the workpiece surface and their contribution to the contact tribology beyond dry-machining at high vacuum. For this purpose the spaces above workpiece and tool surfaces need to be filled with particles that follow fluid particle dynamics.

Figure 1.10 shows some details of the design of the 3D simulation cell, which is identical to those in Figures 1.4 to 1.8, except for the atomic fluid and the cut depth, which was chosen as $a_e = 0.5$ nm (like in Figure 1.6). The cutting speed was 100 m/s, also as in previous figures. The fluid filled the space above the workpiece surface and around the tool. As a modeling approach, a simple, atomic, non-reacting fluid was considered. The data for the fluid were derived from those of water with a density of 1.0 g/cm^3 and molar mass of 18 g, which results in a fluid mass of $2.988*10^{-26}$ kg and average bonding distance of 0.3154 nm. The atomic approach ignores the rotational molecular moments of inertia and reduces its mass to the center of gravity. The data for the molecule-molecule interaction energy of water were found in [RAP 95]. The fluid-fluid interactions as well as the tool (hard)-workpiece interactions were calculated on the basis of the Lennard-Jones (LJ) potential function. The wetting of the tool (fluid-tool) and workpiece surface (fluid-workpiece) were also described by the fluid-fluid potential function that represents a weak interaction like hydrogen bonding in water, but no chemical reaction. As the consideration of a fluid in the cutting process simulation was the focus of this work, internal tool dynamics were not considered here. For the inner workpiece reactions an EAM was applied (copper [ACK 87]). The data for the tool-workpiece interaction represent a friction contact in diamond cutting with suitable lattice constant and cut-off distance [IKA 91].

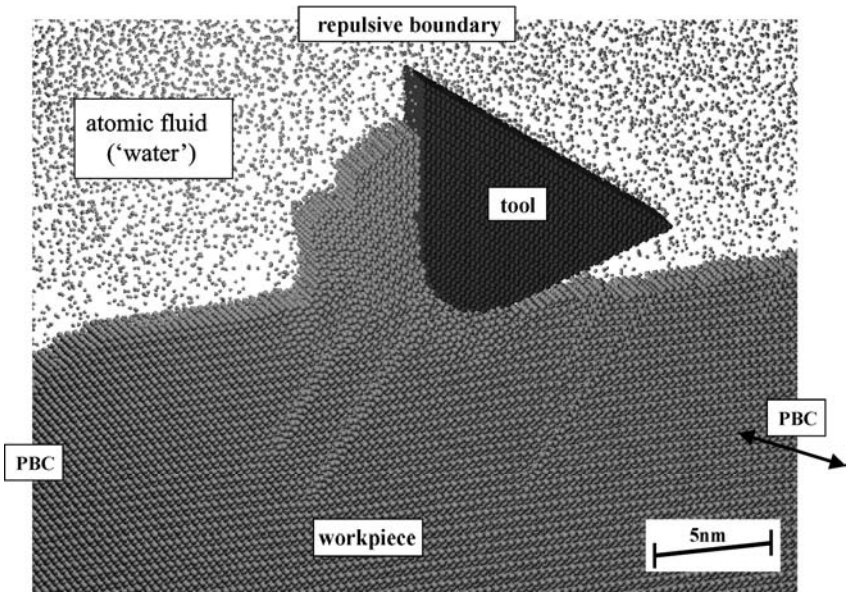

Figure 1.10. *Snapshot of an MD-cutting simulation considering an atomic fluid (after 600,000 time steps, 240 ps)*

By adding only the fluid to the MD model, a direct comparison with earlier results is possible and the impact of the fluid on the material removal process simulation can clearly be pointed out. Figure 1.11 shows the impact of the fluid on the chip formation and Figure 1.12 shows the effect on the temperature distribution.

In both simulations in Figure 1.11 the tool was initially not in contact with the workpiece, and followed the same trajectory and cut for about the same distance as the workpiece. With the presence of the fluid the material removal process starts earlier and the chip formation appears more efficient, since more material is piled up at the rake face of the tool. Thus, at vacuum condition (no fluid), more material is drawn underneath the tool tip, for which the workpiece must store higher elastic stress and more elastic deformation below the tool than with the fluid atmosphere. This phenomenon is closely related to the workpiece surface stresses which will be reduced by the interaction with the fluid atoms.

It is interesting to notice that the fluid density is lower at the workpiece surface, where the fluid atoms pick up heat from the heavier and thermally active (freely vibrating) workpiece atoms. At the same time, the tool atoms were not vibrating, i.e. they could not exchange heat with the fluid atoms. As a consequence, many fluid atoms adhered to the tool surface and formed a fluid layer (see Figure 1.11a).